The product of *uncI* gene in F_1F_o-ATP synthase operon plays a chaperone-like role to assist *c*-ring assembly

Toshiharu Suzuki*†, Yoko Ozaki†, Nobuhito Sone*, Boris A. Feniouk†, and Masasuke Yoshida*†‡

*ATP Synthesis Regulation Project, ICORP, Japan Science and Technology Corporation, Aomi 2-41, Tokyo 135-0064, Japan; and †Chemical Resources Laboratory, Tokyo Institute of Technology, Nagatsuta 4259, Yokohama 226-8503, Japan

Edited by H. Ronald Kaback, University of California, Los Angeles, CA, and approved October 30, 2007 (received for review August 27, 2007)

Bacterial operons for F_1F_o-ATP synthase typically include an *uncI* gene that encodes a function-unknown small hydrophobic protein. When we expressed a hybrid F_1F_o (F_1 from thermophilic *Bacillus* PS3 and Na^+-translocating F_o from *Propionigenium modestum*) in *Escherchia coli* cells, we found that *uncI* derived from *P. modestum* was indispensable to produce active enzyme; without *uncI*, *c*-subunits in F_1F_o existed as monomers but not as functional c_{11}-ring. When *uncI* was expressed from another plasmid at the same time, active F_1F_o with c_{11}-ring was produced. A plasmid containing only *uncI* and *c*-subunit gene produced c_{11}-ring, but a plasmid containing only *c*-subunit gene did not. Direct interaction of UncI protein with *c*-subunits was suggested from copurification of His-tagged UncI protein and *c*-subunits, both in the state of c_{11}-ring and *c*-monomers. Na^+ induced dissociation of His-tagged UncI protein from c_{11}-ring but not from *c*-monomers. These results show that UncI is a chaperone-like protein that assists c_{11}-ring assembly from *c*-monomers in the membrane.

protein folding | membrane protein | Na^+ transport

F_1F_o-ATP synthase (F_1F_o) is located in membranes of mitochondria and chloroplast thylakoid, and cytoplasmic membranes of bacteria, and it couples ATP synthesis/hydrolysis with transmembrane H^+ or Na^+ translocation (1, 2). F_1F_o is composed of two domains, water-soluble F_1 that has nucleotide-binding sites for ATP synthesis/hydrolysis, and membrane-integral F_o that mediates H^+ translocation across the membrane. In the case of the simplest bacterial F_1F_o, subunit compositions of F_1 and F_o are $\alpha_3\beta_3\gamma\delta\varepsilon$ and $a_1b_2c_{10-15}$, respectively. In F_o, the *c*-subunit takes a simple hairpin-like structure composed of two transmembrane helices (3), and multimeric *c*-subunits assemble into a ring architecture (*c*-ring), where the number of *c*-subunits differs in a range of 10–15 depending on the sources (4–7). F_1F_o is a rotary motor enzyme in which a rotor composed of $\gamma\varepsilon c_{10-15}$ rotates relative to a stator moiety of $\alpha_3\beta_3\delta ab_2$ (8, 9). Downhill H^+ flow through F_o drives rotation of the *c*-ring and hence a whole rotor, which induces sequential conformational changes of catalytic sites of F_1 domain that result in ATP synthesis (10). In the reverse reaction, ATP hydrolysis at the F_1 domain drives rotation of the γ-subunit and hence a whole rotor, which drives pumping H^+ across membrane at the F_o domain. Structural studies revealed gearwheel-like architectures of chloroplast c_{14}-ring (7) and *Ilyobactor tartaricus* c_{11}-ring (11). In *I. tartaricus* and *Propionigenium modestum* F_1F_os, the c_{11}-ring is highly stable (even in SDS solution), and a strong acid-denaturant, trichloroacetic acid, is necessary to break the ring (12, 13). Although the c_{11}-ring structure is highly stable, it cannot be spontaneously formed from *c*-subunit monomers; when *P. modestum uncE* (encoding the *c*-subunit) was solely expressed in *Escherichia coli* cells, c_{11}-ring was not formed (14).

In 1981, Gay and Walker (15, 16) determined the structure of *E. coli unc* operon for F_1F_o that contained nine open reading frames (*uncIBEFHAGDC*) in which *uncB*, *E*, *F*, *H*, *A*, *G*, *D*, and *C* encode *a*-, *c*-, *b*-, δ-, α-, γ-, β-, and ε-subunits, respectively. The *uncI* encodes a 14-kDa hydrophobic protein that is not a component of F_1F_o, possibly corresponding to the unidentified protein synthesized by *in vitro* transcription–translation from a plasmid containing whole *unc* operon (17). The authors speculated that it must be a "pilot protein" necessary for F_1F_o assembly. Later analysis confirmed that the *unc* promoter is located in front of *uncI* (18, 19), and therefore, *uncI* is indeed a member of the *unc* operon. However, *uncI* gene product protein (UncI) was not found in *E. coli* cells under the normal growth condition, and disruption of the *uncI* gene by insertions (20) or deletion (21) caused no significant effect on the functions of F_1F_o, although growth yield was lowered. The UncI protein was detected later in *E. coli* minicells by using strong expression vectors (19, 22). Immunoblot analysis using anti-UncI antibody revealed the presence of UncI in preparations of F_o and F_1F_o, although the amounts were far less than stoichiometric level (23, 24). Consistent with its high hydrophobicity predicted from the nucleotide sequence, UncI was purified by chloroform/methanol extraction (22). Despite of the accumulated information on UncI, its role remains unclear.

Although F_1F_o from most organisms is a highly specific H^+ pump, in some bacteria such as *P. modestum*, it operates on Na^+ (25). In an attempt to make a hybrid F_1F_o (F_1 from *Bacillus* PS3 and F_o from *P. modestum*) in *E. coli* cells, we found the essential role of *uncI* to produce active hybrid F_1F_o. The results show that UncI is a molecular chaperone-like protein that assists the *c*-ring assembly.

Results

Hybrid F_1F_o Was Expressed in *E. coli*. Both *P. modestum* and thermophilic *Bacillus* PS3 have a typical bacterial *unc* operon with nine genes in the order of *uncIBEFHAGDC* (26, 27). The hybrid F_1F_o, composed of *Bacillus* PS3 F_1 and *P. modestum* F_o, was generated by connecting *P. modestum uncIBEF'* and *Bacillus* PS3 *uncF'HAGDC*. In bacterial F_1F_os, the *b*-subunit has four domains: transmembrane, tether, dimerization, and δ-binding (28). Genetic connection to generate hybrid F_1F_o was made at the region coding for the dimerization domain (position 73–74; *P. modestum* numbering) because this region has been assumed to have no interaction with other subunits. An F_1F_o-deficient *E. coli* strain JM103Δ*unc* was transformed with a pTR-$hF_1F_o^{(+i)}$, an expression vector for the hybrid F_1F_o. SDS/PAGE analysis showed expression of F_1F_o in the membrane fraction of the host *E. coli* cells (Fig. 1*A*, lane 2). The expressed F_1F_o [termed $hF_1F_o^{(+i)}$ hereafter] has a histidine tag at the N terminus of β-subunit and therefore, could be purified to homogeneity by Ni-nitrilotriacetic acid (Ni-NTA) affinity chromatography after solubilization with Triton X-100 (Fig. 1 *A*, lane 1, and *B*, lane 9). N-terminal sequencing of the bands in the gel confirmed the

Author contributions: T.S. and M.Y. designed research; T.S., Y.O., N.S., and B.A.F. performed research; T.S. analyzed data; and T.S. and M.Y. wrote the paper.

The authors declare no conflict of interest.

This article is a PNAS Direct Submission.

‡To whom correspondence should be addressed at: Chemical Resouces Laboratories, Tokyo Institute of Technology, Nagatsuta 4259, Yokohama 226-8503, Japan. E-mail: myoshida@res.titech.ac.jp.

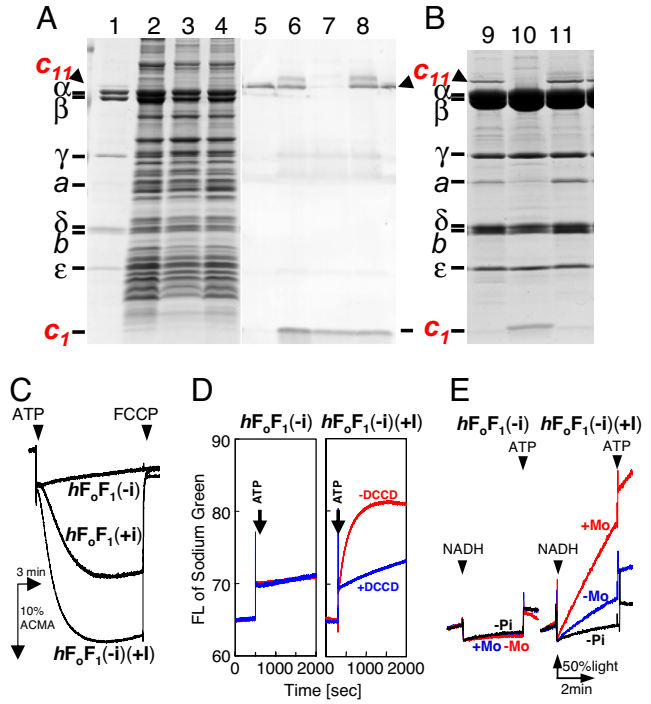

Fig. 1. Assembly of c_{11}-ring in hybrid F_1F_o assisted by *uncI* expressed in another plasmid and activities of the hybrid F_1F_o thus made. Membrane fractions prepared from *E. coli* cells expressing the indicated plasmids (*A*) and purified hybrid F_1F_os (*B*) were subjected to SDS/PAGE and stained with CBB (*A*, lanes 1–4, and *B*) or immnoblot staining with anti-*c*-subunit antibody (*A*, lanes 5–8). Lanes 1, 5, and 9, purified $hF_1F_o^{(+i)}$ as a reference. Lanes 2 and 6, pTR-$hF_1F_o^{(+i)}$. Lanes 3 and 7, pTR-$hF_1F_o^{(-i)}$. Lanes 4 and 8, pTR-$hF_1F_o^{(-i)}$ ± pST-I. Lane 10, $hF_1F_o^{(-i)}$. Lane 11, $hF_1F_o^{(-i)(+i)}$. (*A*) Membrane proteins (7 μg) were applied to each lane of the gels. (*C*) H^+-pumping activities of PLs containing hybrid F_1F_os, $hF_1F_o^{(+i)}$, $hF_1F_o^{(-i)}$, or $hF_1F_o^{(-i)(+i)}$. (*D*) Na^+-pumping activity of PLs containing $hF_1F_o^{(-i)}$ and $hF_1F_o^{(-i)(+i)}$. (*E*) ATP synthesis activity of membrane vesicles containing $hF_1F_o^{(-i)}$ and $hF_1F_o^{(-i)(+i)}$. (*C–E*) Experimental conditions were the same as in Fig. 2. Fifty percent light in *E* corresponds to half of the initial luminescence intensity in the cuvette before the addition of NADH.

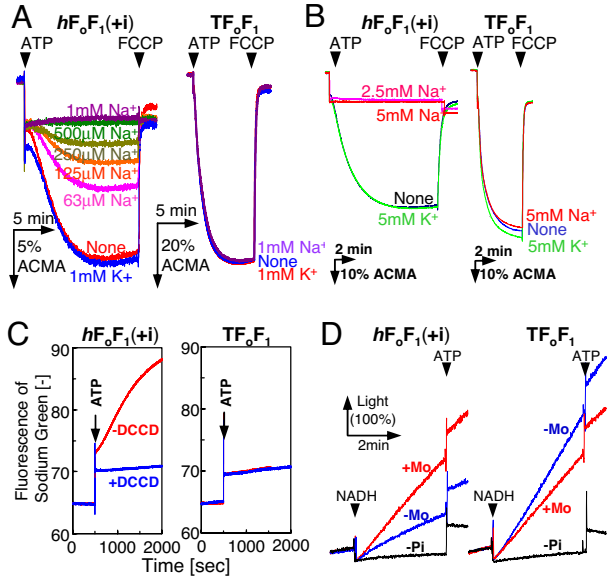

Fig. 2. Activities of the hybrid F_1F_o (*Left*) compared with TF_1F_o (*Right*). (*A*) H^+-pumping activity of inverted *E. coli* membrane vesicles containing the hybrid F_1F_o [$hF_1F_o^{(+i)}$] and TF_1F_o. NaCl or KCl was added into the assay mixture at the concentrations indicated. The reaction was initiated by adding 1 mM K^+-ATP and terminated with FCCP. %ACMA shows the fluorescent intensity of ACMA, in which the initial intensity before the addition of ATP is calibrated as 100%. (*B*) H^+-pumping activity of PLs containing $hF_1F_o^{(+i)}$ and TF_1F_o. The assay conditions were the same as *A*. (*C*) Na^+-pumping activity of PLs containing $hF_1F_o^{(+i)}$ and TF_1F_o. As indicated, PLs were reacted with 50 μM DCCD for 1 h and used for the measurement. The reaction was initiated by the addition of 1.3 mM Na^+_2-ATP, and the increase in Na^+ concentration inside the PLs was monitored with an increase in sodium green fluorescence at 540 nm. (*D*) ATP synthesis activity of membrane vesicles containing $hF_1F_o^{(+i)}$ and TF_1F_o. Electrochemical potential of H^+ was generated by respiratory H^+ pumps in the membrane vesicles driven by NADH oxidation. ATP synthesis was monitored in real time at 35°C by luciferase reaction at 560 nm. As indicated, a Na^+/H^+ antiporter, monensin (5 μM) was added to convert some amount of H^+ gradient into Na^+ gradient. Traces indicated by ''-Pi'' represent negative controls without addition of P_i. Light (100%) in *D* corresponds to the initial luminescence intensity in the cuvette before the addition of NADH.

expression of all F_1F_o subunits except the *a*-subunit. The *a*-subunit band was identified by immunoblot analysis using anti-*a* antibody (data not shown) because of the difficulty of N-terminal sequencing of the *a*-subunit. As reported for *P. modestum* F_o[§] (12), a high-molecular-mass band (≈60 kDa) was observed above the α-subunit band (indicated by c_{11} and an arrowhead in the figure). N-terminal sequencing gave a *c*-subunit sequence, and the band disappeared by treating the sample with trichloroacetic acid before electrophoresis (data not shown), confirming that this band corresponded to the c_{11}-ring as in the case of *P. modestum* F_1F_o.

Hybrid F_1F_o Can Use Na^+ as a Coupling Ion. We examined the activities of $hF_1F_o^{(+i)}$ in the membrane vesicles prepared from expressing *E. coli* cells (Fig. 2 *A* and *D*) and in the proteoliposomes (PLs) (Fig. 2 *B* and *C*). Activities of *Bacillus* PS3 F_1F_o (TF_1F_o) were shown as references (Fig. 2 *A–D*, *Right*). The $hF_1F_o^{(+i)}$ exhibited H^+-pumping activity upon addition of ATP in the absence of Na^+, but not in the presence of 1 mM NaCl (Fig. 2*A*, *Left*). KCl at 1 mM had no effect. Titration of Na^+ concentration indicated that approximately half of the H^+-pumping activity was blocked by supplementing 0.2 mM NaCl. The inhibition of H^+ pumping by Na^+ was also observed for the purified $hF_1F_o^{(+i)}$ in PLs (Fig. 2*B*, *Left*). The apparent inhibition of H^+ pumping could be explained by increasing Na^+ pumping as Na^+ became available. The H^+-pumping activity of TF_1F_o, on the contrary, was unaffected by the presence of NaCl and KCl (Fig. 2 *A* and *B*, *Right*). Na^+-pumping activity was measured directly with a Na^+-indicator fluorescent dye, sodium green (Fig. 2*C*). In the presence of 2.6 mM NaCl, $hF_1F_o^{(+i)}$ pumped Na^+ upon addition of ATP, and this activity was totally lost by prior incubation with dicyclohexylcarbodiimide (DCCD) (Fig. 2*C*, *Left*). Such Na^+-pumping activity was not observed for PLs of TF_1F_o (Fig. 2*C*, *Right*). When the electrochemical potential of H^+ was generated by respiratory proton pumps fueled by NADH, $hF_1F_o^{(+i)}$ in the membrane vesicles synthesized ATP (Fig. 2*D*, *Left*). The vesicles showed the ATP synthesis activity of 3.4 milliunits/mg membrane protein in the presence of 2.5 mM NaCl (only outside the vesicles). The activity was increased 2.1-fold by the addition of a Na^+/H^+ antiporter, monensin (5 μM), which exchanged H^+ inside the vesicle and Na^+ outside the vesicles, transforming a significant magnitude of ΔpH into ΔpNa (Fig. 2*D*, *Left*). The vesicles containing TF_1F_o synthesized ATP at a rate 17.6 milliunits/mg membrane proteins, and this activity decreased to ≈60% by monensin, likely because of the decrease

[§]In a report of *P. modestum* F_1F_o (12), a band of c_{11}-ring in SDS/PAGE was observed just below β-subunit, not above α-subunit as observed here. The difference is a result of the gel used. We used gradient gels (10–20% polyacrylamide) in this work. When gels with constant polyacrylamide concentration were used, the band was observed below β-subunit.

in ΔpH (Fig. 2*D*, *Right*). ATP hydrolysis activity of $h\mathrm{F_1F_o}^{(+i)}$ in PLs was 1.2 units/mg of $\mathrm{F_1F_o}$ in the absence of $\mathrm{Na^+}$. This activity was enhanced 4-fold by the addition of 5 mM NaCl (apparent K_m value for $\mathrm{Na^+}$ = 0.7 mM at 42°C) as reported (12, 29). These results suggested that $h\mathrm{F_1F_o}^{(+i)}$ is very similar to the authentic *P. modestum* $\mathrm{F_1F_o}$ in its $\mathrm{Na^+}$ dependence (29, 30).

***uncI* Is Necessary for c_{11}-Ring Formation in Hybrid $\mathrm{F_1F_o}$.** To determine the function of *uncI*, we removed the *uncI* gene from the plasmid pTR-$h\mathrm{F_1F_o}^{(+i)}$ and generated an expression plasmid pTR-$h\mathrm{F_1F_o}^{(-i)}$. Also, we generated an expression plasmid pST-I that contained only *uncI* gene. Membrane fractions of *E. coli* cells transformed by pTR-$h\mathrm{F_1F_o}^{(+i)}$, by pTR-$h\mathrm{F_1F_o}^{(-i)}$, and by pTR-$h\mathrm{F_1F_o}^{(-i)}$ ± pST-I were analyzed with SDS/PAGE (Fig. 1*A*). They all produced $\mathrm{F_1F_o}$s as demonstrated by appearance of the bands of α- and β-subunits in SDS/PAGE of membrane fractions (lanes 2–4). The immunoblot analysis by anti-*c* antibody revealed that c_{11}-ring was present in membrane fractions from cells expressing pTR-$h\mathrm{F_1F_o}^{(+i)}$ (lane 6) and pTR-$h\mathrm{F_1F_o}^{(-i)}$ + pST-I (lane 8) but not in those from cells expressing pTR-$h\mathrm{F_1F_o}^{(-i)}$ (lane 7), whereas *c*-monomer existed in all cases. The hybrid $\mathrm{F_1F_o}$s were purified to homogeneity and analyzed with SDS/PAGE. In SDS/PAGE analysis (Fig. 1*B*), the band of *c*-subunit appeared at the position of monomer in the case of $\mathrm{F_1F_o}$ produced from pTR-$h\mathrm{F_1F_o}^{(-i)}$ [termed $h\mathrm{F_1F_o}^{(-i)}$] (lane 10) but at the position of the c_{11}-ring in $h\mathrm{F_1F_o}^{(+i)}$ (lane 9) and in $\mathrm{F_1F_o}$ produced from pTR-$h\mathrm{F_1F_o}^{(-i)}$ ± pST-I [termed $h\mathrm{F_1F_o}^{(-i)(+\mathrm{I})}$] (lane 11). Because $\mathrm{F_1F_o}$s had a histidine tag at N termini of β-subunits and were purified by Ni-NTA affinity chromatography, *c*-subunits running as a monomer in SDS/PAGE should be components of the $h\mathrm{F_1F_o}^{(-i)}$. Although it is not known whether these *c*-subunits exist as monomers or as loosely associated oligomers in $h\mathrm{F_1F_o}^{(-i)}$, we call them "monomers" hereafter for simplicity. Comparison of immunoblot analysis (Fig. 1*A*, lanes 6 and 8) with protein staining of the purified $\mathrm{F_1F_o}$s (Fig. 1*B*, lanes 9 and 11) suggested that *c*-monomers in membrane fractions of cells expressing pTR-$h\mathrm{F_1F_o}^{(+i)}$ and those expressing pTR-$h\mathrm{F_1F_o}^{(-i)}$ + pST-I would be free, which indicates that they were not incorporated into $\mathrm{F_1F_o}$ complex and were removed during purification procedures. It was noticed that $h\mathrm{F_1F_o}^{(-i)}$ lost a significant amount of *a*-subunit (Fig. 1*B*, lane 10). These results clearly indicate that *uncI*, either in the same *unc* operon or in a different transcript, is necessary for assembly of the c_{11}-ring. It should be noted that genomic DNA of the JM103Δ*unc* strain lacks all of the structural genes for $\mathrm{F_1F_o}$ but has an *uncI* gene of its own. However, it is clear from the results described above that the *E. coli uncI* gene cannot complement the *P. modestum uncI* gene.

Hybrid $\mathrm{F_1F_o}$ Containing No c_{11}-Ring Is Inactive. The purified $\mathrm{F_1F_o}$s were incorporated into liposomes, and activities were measured. $h\mathrm{F_1F_o}^{(-i)}$ was inactive in $\mathrm{H^+}$ pumping (Fig. 1*C*), $\mathrm{Na^+}$ pumping (Fig. 1*D*), and ATP synthesis (Fig. 1*E*). In contrast, $h\mathrm{F_1F_o}^{(-i)(+\mathrm{I})}$ showed good activities in all measurements. Actually, its $\mathrm{H^+}$-pumping activity was higher than that of $h\mathrm{F_1F_o}^{(+i)}$ (Fig. 1*C*). $\mathrm{Na^+}$-pumping activity of $h\mathrm{F_1F_o}^{(-i)(+\mathrm{I})}$ was sensitive to DCCD inactivation, and ATP synthesis was activated up to 5.1 milliunits/mg membrane proteins by monensin (Fig. 1 *D* and *E*).

UncI Can Assist c_{11}-Ring Assembly Independent of Other Subunits of $\mathrm{F_1F_o}$. Three kinds of plasmids were made: pTR-*c* for expression of *c*-subunit, pST-$\mathrm{I_{His}}$ for expression of $\mathrm{UncI_{His}}$ protein with a His tag at the C terminus, and pTR-$\mathrm{I_{His}}$*c* for expression of $\mathrm{UncI_{His}}$ protein and *c*-subunit (Fig. 3). Membrane fractions from cells expressing pTR-$\mathrm{I_{His}}$*c* contained c_{11}-ring (lane 2), whereas those from cells harboring pTR-*c* contained no c_{11}-ring (lane 3). The *c*-monomer band was also faint in lane 3. It seems that in the absence of interactions with UncI and other subunits of $\mathrm{F_1F_o}$, newly synthesized *c*-subunit is unstable. As expected from the result of $h\mathrm{F_1F_o}^{(-i)(+\mathrm{I})}$, c_{11}-ring was formed even when a gene for *c*-subunit and the *uncI* gene were on the different plasmids (pTR-*c* and pST-$\mathrm{I_{His}}$), although the amount was relatively small (lane 4). These results suggest that the UncI protein can assist assembly of *c*-monomers into c_{11}-ring without the involvement of other subunits of $\mathrm{F_1F_o}$.

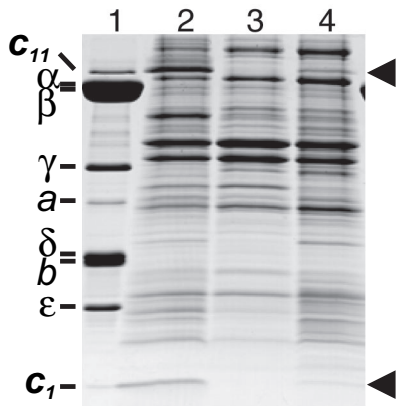

Fig. 3. c_{11}-ring formation assisted by *uncI* without involvement of other subunits of $\mathrm{F_1F_o}$. SDS/PAGE of membrane fractions prepared from cells expressing pTR-$\mathrm{I_{His}}$*c* (lane 2), pTR-*c* (lane 3), and pTR-*c* + pST-$\mathrm{I_{His}}$ (lane 4). Lane 1, purified $h\mathrm{F_1F_o}^{(+i)}$ as a reference. Membrane proteins (7 μg) were applied to each lane of the gels. Bands of c_{11}-ring and *c*-monomer are indicated with arrowheads. It should be noted that expression of UncI from pST-$\mathrm{I_{His}}$ is weaker than that from pTR-$\mathrm{I_{His}}$*c* because of a weaker transcription promoter.

UncI Protein Interacts Directly with *c*-Subunit. The above results suggest a possibility of interaction of UncI protein with *c* subunit. *E. coli* cells expressing pTR-$\mathrm{I_{His}}$*c* contained c_{11}-ring (Fig. 4*A*, lane 2) as shown above, which was solubilized by Triton X-100 (Fig. 4*A*, lane 3). Solubilized proteins were applied to a Ni-NTA column, and, after washing the column, the proteins retained in the column were eluted by the high-imidazole buffer. The eluate contained several protein bands in SDS/PAGE (Fig. 4*A*, lane 4). From N-terminal amino acid sequencing, a 15-kDa protein band was identified as $\mathrm{UncI_{His}}$ and two bands below it as proteolysed products of $\mathrm{UncI_{His}}$. Bands at ≈60 kDa and at 7 kDa gave the sequence of *c*-subunit, and treatment with 10% trichloroacetic acid converted the ≈60-kDa band to the 7-kDa band (Fig. 4*A*, lane 5). Therefore, they certainly corresponded to c_{11}-ring and *c*-monomer. The fact that the c_{11}-ring and *c*-monomer were copurified with $\mathrm{UncI_{His}}$ substantiates direct interaction between UncI and *c*-subunit, either in the state of c_{11}-ring or *c*-monomer. UncI assists the ring assembly of *c*-subunits through a direct protein–protein interaction.

$\mathrm{Na^+}$ Induces Dissociation of UncI from c_{11}-Ring. In this work, all experimental procedures, unless otherwise stated, were carried out under the conditions where $\mathrm{Na^+}$ was strictly omitted. To know the effect of $\mathrm{Na^+}$ on the UncI–*c*-subunit interaction, the Ni-NTA column, to which Triton X-100-solubilized membrane proteins from cells expressing pTR-$\mathrm{I_{His}}$*c* were loaded, was washed with a $\mathrm{Na^+}$-containing washing buffer. Then, the proteins were eluted out with the high-imidazole buffer, and the eluate was analyzed directly by SDS/PAGE with silver staining. As seen, the eluate contained only *c*-monomer (Fig. 4*B*, lane 7), indicating that c_{11}-ring was already washed out from the column during the wash with the $\mathrm{Na^+}$-containing washing buffer. In a control experiment where the column was washed with a ($\mathrm{Na^+}$-free) washing buffer, the eluate contained c_{11}-ring and *c*-monomer (Fig. 4*B*, lane 6), as observed in the previous

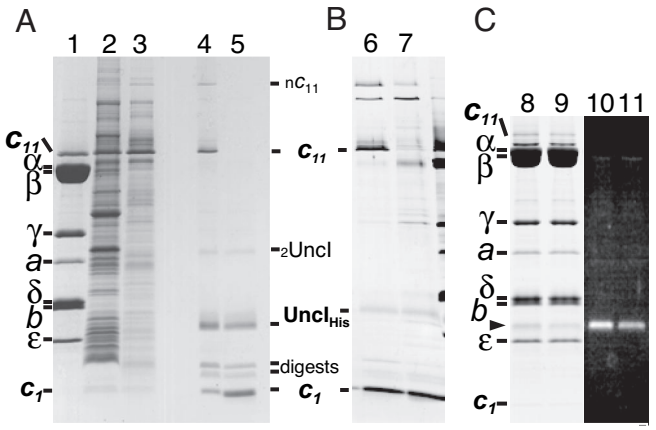

Fig. 4. Association of UncI protein with *c*-subunit and release of c_{11}-ring from UncI by Na^+. (*A*) SDS/PAGE analysis of $UncI_{His}$-bound components. Lane 1, $hF_1F_o^{(+i)}$. Membrane fractions of cells expressing pTR-$I_{His}c$ (lane 2) were solubilized with Triton X-100. Solubilized proteins were isolated by ultracentrifugation (lane 3) and loaded on a Ni-NTA column. After washing the column, the proteins were eluted (lane 4), and the eluate was further treated with 10% trichloroacetic acid (lane 5). All of the buffers did not contain Na^+. nc_{11}, aggregated c_{11}-ring; $2UncI_{His}$, dimer $UncI_{His}$; digests, proteolytic products of $UncI_{His}$. Proteins on the gel were stained by Coomassie brilliant blue (CBB). (*B*) Effect of Na^+ on the interaction between $UncI_{His}$ and *c*-subunit. The eluate from the Ni-NTA column was directly subjected to SDS/PAGE without prior concentration procedures, and the proteins were stained with silver staining. $UncI_{His}$ was only poorly stained by silver. Lane 6, the same as lane 4. Lane 7, the loaded Ni-NTA column was washed with the Na^+-containing washing buffer (containing 100 mM NaCl) and eluted. (*C*) Detection of UncI in $hF_1F_o^{(-i)(+I)}$. Membrane fractions of cells expressing pTR-$hF_1F_o^{(-i)}$ ± pST-I were solubilized and loaded on a Ni-NTA column. The column was washed with the (Na^+-free) washing buffer (lanes 8 and 10) or with the Na^+-containing washing buffer (lanes 9 and 11). The $hF_1F_o^{(-i)(+I)}$ was eluted, reacted with tetramethylrhodamine maleimide to label cysteine residues in UncI, and subjected to SDS/PAGE analysis. The proteins were visualized by CBB staining (lanes 8 and 9) or by fluorescence (excited at 302 nm, emission at >400 nm) (lanes 10 and 11). UncI proteins are indicated with arrowheads. Different from the gel in Fig. 1*B*, the band of UncI was visible even by CBB staining because the fluorescent dye labeling enhanced the sensitivity of UncI to the CBB staining.

experiment (Fig. 4*A*, lane 4). The band of $UncI_{His}$ was faint because it was stained only poorly by silver. These results suggest that Na^+ induces dissociation of UncI from c_{11}-ring but not from *c*-monomer.

As shown in Fig. 1*B* (see lanes 9 and 11), UncI protein was not found in the purified hybrid F_1F_o, and it is clear that UncI is not a stable component of the mature enzyme. However, weak, substoichiometric association of UncI to F_1F_o has been reported for *E. coli* F_1F_o (23, 24). To analyze such UncI–F_1F_o interaction, we took advantage of the fact that hybrid F_1F_o does not have cysteine residue, but UncI has three. $hF_1F_o^{(-i)(+I)}$ was adsorbed to the Ni-NTA column through the His tag at the β-subunits, and the column was washed with either Na^+-free or Na^+-containing washing buffer. Then, the bound proteins were eluted by the high-imidazole buffer and analyzed by SDS/PAGE after treatment with a cysteine-reactive fluorescence dye, tetramethylrhodamine maleimide. In the protein-staining gel, the UncI band was seen faintly in Na^+-unexposed $hF_1F_o^{(-i)(+I)}$ but hardly seen in Na^+-exposed $hF_1F_o^{(-i)(+I)}$ (Fig. 4*C*, lanes 8 and 9). Consistently, fluorescence intensity of the UncI band was 1.4 (±0.1)-fold weaker in Na^+-exposed $hF_1F_o^{(-i)(+I)}$ than in Na^+-unexposed $hF_1F_o^{(-i)(+I)}$ (Fig. 4*C*, lanes 10 and 11). Although the amount of associated UncI decreased by Na^+, a small amount of UncI still remained on F_1F_o preparation.

Discussion

Ever since *uncI* gene was found 26 years ago (15, 16), its function has been elusive. It occupies the first position in the *unc* operon

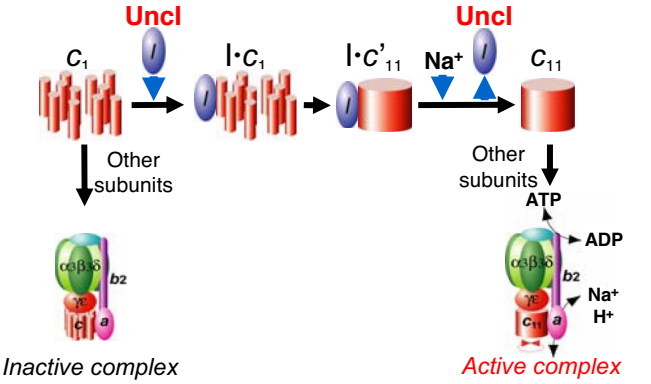

Fig. 5. A model of UncI-assisted assembly of c_{11}-ring. UncI binds to monomer (or some unassembled state of) *c*-subunit(s) in the membranes, assists their assembly into c_{11}-ring, and leaves c_{11}-ring as Na^+ binds to c_{11}-ring. Other subunits associate with c_{11}-ring, and active F_1F_o is formed. Without UncI, an inactive F_1F_o complex is formed. In this complex, *c*-subunits are not assembled into c_{11}-ring, and some fraction of *a*-subunit is lost. c'_{11} indicates an interim state of c_{11}-ring formation.

and is conserved in most bacteria, indicative of its importance. This work reveals an essential role of UncI protein for the ring assembly of *c*-subunits of *P. modestum* F_o (Fig. 5). In mitochondrial F_1F_o, some proteins, such as yeast ATP10 (31, 32), ATP23 (33, 34), and OXA1 (35), have been shown to play a chaperone-like role to assist F_o assembly, although the detailed mechanism is not well understood. Although there is no sequence homology to eukaryotic proteins, UncI protein also plays a chaperone-like role; it associates with monomers of *c*-subunit, assists ring assembly, and dissociates from the assembled *c*-ring. Because molecular chaperone is not a final component of the mature protein (complex), it should leave its client protein at some stage either by using energy of ATP hydrolysis, by other factor(s), or just by reversible association/dissociation. UncI dissociates from *c*-ring but not from *c*-monomers in the presence of Na^+ ion, thus "catalyzing" a forward reaction, assembling the ring. Because Na^+ is a transporting ion for *P. modestum* F_o, binding of Na^+ to the *c*-ring would be responsible for this reaction. This work also revealed that *c*-subunits that fail to form the functional ring can be incorporated into F_1F_o complex, although the resultant F_1F_o is inactive in coupling reactions. It awaits further study whether this inactive F_1F_o is a dead-end complex or can be a precursor of an active F_1F_o. Possibly related to this finding, a small amount of UncI protein remains bound in the purified $hF_1F_o^{(-i)(+I)}$, especially in the Na^+-unexposed F_1F_o. This UncI could be associated with a small population of *c*-ring or of residual *c*-monomers in the complex. UncI protein has been found in mature *E. coli* F_1F_o (23), and a possibility of interaction between UncI and F_o subunits other than *c*-subunit (24) is not eliminated by this work.

A proposal of UncI function as an essential factor to assemble *c*-ring will raise immediate questions: why can an *E. coli* mutant that lacks *uncI* gene grow by oxidative phosphorylation, and why is F_1F_o isolated from the mutant fully active (20, 21)? It is possible that chaperone-like function of UncI is restricted only in the case of *P. modestum* F_o. However, nonessential phenotype of *E. coli uncI* gene might be explained by another chaperone-like protein for membrane proteins in *E. coli*, YidC. Recent analysis of membrane-integration process of *E. coli c*-subunit showed that newly translated *c*-subunit is targeted by the signal recognition particles to the membranes and integrated into membranes by the assist of YidC (36). It was further demonstrated that YidC had an ability to assist the ring formation from

BIOCHEMISTRY

c-monomers (37). Therefore, it is likely that YidC has an overlapping function with UncI and can complement the UncI deficiency. Such a role of YidC might be specific to *E. coli* *c*-ring and cannot assist *P. modestum* c_{11}-ring assembly as implicated by this work.

Finally, aside from UncI issue, it is worth pointing out that the same F_1 domain derived from a thermophilic *Bacillus* can dock with c_{11}-ring in the hybrid as well as with c_{10}-ring in the original TF_1F_o. An analogous result has been also observed for another hybrid F_1F_o, which is composed of *E. coli* F_1 and *P. modestum* F_o (38). It appears that γ- and ε-subunits of thermophilic *Bacillus* F_1 can manage to bind a *c*-ring with a slightly larger radius to make a body of rotor apparatus that is robust enough to transmit the large rotary torque between F_o and F_1.

Materials and Methods

Expression Vectors for Hybrid F_1F_o. A DNA fragment, containing *uncIBE* and the 5′ half of *uncF*, was amplified from *P. modestum* genomic DNA by PCR. A DNA fragment, containing the 5′ half of *uncF* and *uncHA*′ was amplified by PCR from an expression plasmid for *Bacillus* PS3 F_1F_o (TF_1F_o), pTR19-ASDS (termed pTR-TF_1F_o in this work) (10). The two fragments possess the same nucleotide sequence at the edge (*b*-subunit region), and therefore, the fragments were connected by PCR amplification without an additional primer. The resulting fragment composed of *P. modestum uncIBEF*′ and *Bacillus* PS3 *unc*′*FA*′ was digested with EcoRI and KpnI and replaced with the corresponding region of pTRN-ASDS¶ (EcoRI and KpnI sites) to obtain an expression plasmid, pTR-$hF_1F_o^{(+I)}$. Also, pTR-$hF_1F_o^{(-I)}$, in which *uncI* gene was removed from pTR-$hF_1F_o^{(+I)}$, was made to test the role of *uncI*.

Preparation of Membrane Vesicles and the Hybrid F_1F_o. The plasmid pTR-$hF_1F_o^{(+I)}$ was used for transformation of an F_1F_o-deficient *E. coli* strain, JM103Δ(*uncB-uncD*) (hereafter, JM103Δ*unc*) (39). The transformants were aerobically grown in 2×YT medium supplemented with 100 μg/ml ampicillin for 21 h. In the case of transformants harboring pSTV28 derivative plasmid (mentioned later), 30 μg/ml chloramphenicol was also supplemented to maintain the plasmid in the cells. Cells (≈30 g) harvested from a 12-liter culture were washed twice with buffer PA3 [10 mM Hepes/KOH buffer (pH 7.5) containing 5 mM $MgCl_2$ and 10% glycerol] and used for the preparation of inverted membrane vesicles as described in ref. 40 except cell disruption by sonication instead of the French press. Membrane vesicles were used for analyses of F_1F_o. Purification of the hybrid F_1F_o was carried out as follows. The membrane vesicles (≈15 mg of proteins per ml, 16 ml) was washed with 16 ml of 10 mM Hepes/KOH buffer (pH 7.5) and then solubilized in 10 mM Hepes/KOH buffer (pH 7.5) containing 1% Triton X-100 in the presence of a protease inhibitor (Complete EDTA-free; Roche) for 30 min on ice with occasional mixing. After a centrifugation (153,000 × *g*, for 20 min, at 4°C), the supernatant was diluted 4-fold with the buffer M [20 mM potassium phosphate (KP_i)$_i$ buffer (pH 7.5) containing 100 mM KCl] supplemented with 20 mM imidazole. The diluted supernatant was mixed with 12 ml of Ni-NTA Superflow (Qiagen) and calmly stirred for 30 min on ice. The resin was poured onto an appropriate column and washed with 3 vol of the buffer M supplemented with 0.05% Triton X-100 and 20 mM imidazole. F_1F_o was eluted with the buffer M supplemented with 0.05% Triton X-100 and 200 mM imidazole. F_1F_o in the elution was mixed with 50 mM $MgCl_2$ and 2.7% PEG 6000, incubated on ice for 15 min, and collected by ultracentrifugation (153,000 × *g*, for 20 min, at 4°C). The pellet obtained was dissolved in a small volume of 10 mM Hepes/KOH buffer (pH 7.5) containing 0.05% Triton X-100. After a brief centrifugation, the supernatant was frozen by liquid N_2 and stored at −80°C until use. PLs that contained the purified hybrid F_1F_o in the membrane were prepared by the freeze–thaw method as used for TF_1F_o (10).

Expression Vectors for *uncI* and *c*-Subunit. The *uncI* and *uncE* (*c*-subunit gene) were individually amplified by PCR from pTR-$hF_1F_o^{(+I)}$. For Ni-NTA purification of *uncI* gene product, a nucleotide sequence coding for a His tag (6 residues) was introduced in front of the stop codon of *uncI* in the PCR step (termed $uncI_{His}$). The amplified fragments of *uncI* and $uncI_{His}$ were digested with EcoRI and PstI and introduced into the plasmid pSTV28 (Takara) previously digested with both restriction enzymes. The resultant plasmids were named pST-I and pST-I_{His}. By the same manner, the PCR product of *uncE* was introduced into pTrc99A (Amersham Pharmacia) to obtain plasmid pTR-*c*. For simultaneous expression of *uncI* and *uncE*, *uncI* was amplified by PCR, digested with EcoRI and BamHI, and introduced upstream of *uncE* in pTR-*c* to obtain pTR-$I_{His}c$. Nucleotide sequences of the regions amplified by PCR were verified by sequencing. Procedures for cultivation of JM103Δ*unc* transformed with the plasmids, membrane preparation, and membrane solubilization with Triton X-100 were the same as described above for hybrid F_1F_o, but when the A_{600} reached 1, 2 mM isopropyl-β-thiogalactopyranoside was supplemented to the culture. After that, the cultivation was continued for 3 h. Ni-NTA column chromatography was performed as described for hybrid F_1F_o except that (*i*) the Ni-NTA column was washed with 10 bed-vol of the washing buffer [20 mM KP_i buffer (pH 7.5), 100 mM KCl, 30 mM imidazole, and 0.05% Triton X-100] and was eluted with the high-imidazole buffer [20 mM KP_i buffer (pH 7.5), 100 mM KCl, 200 mM imidazole, and 0.05% Triton X-100]; (*ii*) the eluate from the Ni-NTA column was concentrated by a 100-kDa centrifugal concentrator (Ultra YM-100; Amicon) instead of PEG precipitation. In the experiments to test the effect of Na^+ on the UncI–*c*-subunit interaction, the loaded Ni-NTA column was washed with 5 bed-vol of the Na^+-containing washing buffer [20 mM KP_i buffer (pH 7.5), 10 mM KCl, 100 mM NaCl, 30 mM imidazole, 0.05% Triton X-100] and subsequently with 5 bed-vol of the (Na^+-free) washing buffer. Then, the proteins were eluted with the high-imidazole buffer.

Analytical Procedures. ATPase-driven H^+-pumping activity was assayed with quenching of fluorescence of 9-amino-6-chloro-2-methoxyacridine (ACMA) (excitation at 410 nm, emission at 480 nm) at 32°C as described in ref. 10. Inverted membrane vesicles or PLs were added to the assay mixture at a final concentration of 0.2 mg of membrane protein per ml or 20 μg of F_oF_1 per ml. To assess the sensitivity toward Na^+, either NaCl or KCl was supplemented into the assay mixture at the concentration indicated. The reaction was initiated by adding 1 mM K^+-ATP and terminated with 0.25 μg/ml carbonyl cyanide *p*-trifluoromethoxyphenylhydrazone (FCCP). ATPase-driven Na^+-pumping activity was measured by the method of von Ballmoos and Dimroth (41) with some modifications as follows. Soybean L-α-phosphatidylcholine (300 mg, type II-S; Sigma) was suspended by a gentle mixing in 10 ml of buffer PA3 supplemented with 30 μg/ml sodium green (Molecular Probes) and sonicated with a large tip for 30 s. Purified hybrid F_1F_o or TF_1F_o (1 mg) was mixed with 500 μl of the sodium green liposomes, rotated for 5 min at 25°C, frozen with liquid N_2, and thawed on a desk. After water bath sonication (45 s), the PLs were subjected to a cartridge gel filtration column NAP5 (Amersham Pharmacia) previously equilibrated with buffer PA3 to remove the outside sodium green. Thus, prepared PLs were used for the measurement. When indicated, PLs were reacted with 50 μM DCCD in buffer PA3 for 1 h at room temperature before use. Na^+-pumping activity was measured at 32°C in 50 mM Hepes/KOH buffer (pH 7.5) containing 100 mM KCl, 5 mM $MgCl_2$, 4 mM phospho*enol*pyruvate, 0.1 mg/ml pyruvate kinase, and 0.22 ng/ml FCCP in the presence of PLs (final lipid concentration is 3.3 mg/ml). The reaction was initiated by the addition of 1.3 mM Na_2-ATP. The increase in Na^+ concentration inside the PLs was monitored by an increase in fluorescence of sodium green (excitation at 488 nm and emission at 540 nm).

ATP synthesis activity of the membrane vesicles was measured at 35°C in buffer PA3 supplemented with 2.5 mM KP_i, 0.5 mM ADP, 2.5 mM NaCl, membrane vesicles (85 μg and 53 μg of membrane proteins/ml for vesicles containing hybrid F_1F_o and TF_1F_o, respectively), and 1/10 vol of the CLSII solution containing luciferin/luciferase (ATP bioluminescence kit; Roche). If stated, a Na^+/H^+ antiporter, monensin, was supplemented to the solution at a final concentration of 5 μM. The reaction was initiated by adding 1.7 mM NADH to generate electrochemical potential gradient of H^+ across the membrane. The ATP production was monitored in real time by the light from luciferase reaction at 560 nm. The amounts of ATP synthesized were calibrated with a defined amount of ATP at the end of the measurement. The activity that synthesized 1 μmol of ATP per min was defined as 1 unit. ATPase activities were analyzed in 50 mM Hepes/KOH buffer (pH 7.5) containing 100 mM KCl, 5 mM $MgCl_2$, 0.2 μg/ml FCCP, 0.8 mM K^+-ATP, and the ATP-regenerating system (10), and, in the case of membrane vesicles, 2.5 mM KCN to prevent NADH oxidation by *E. coli* respiratory chain. Average hydrolysis rates in a time period from 3 to 6 min after initiation of the reactions at 42°C were measured. The activity that hydrolyzed 1 μmol of ATP per min was defined as 1 unit. Protein concentrations were determined by BCA protein assay kit from Pierce, with BSA as a standard. Fluorescence labeling of UncI in the F_1F_o preparation was performed in 100 mM Mes/KOH (pH 6.5) containing 1% SDS, 1 μg/ml tetramethylrhodamine maleimide (Molecular Probes), and 0.05% Triton X-100 for 30 min at room temperature. All SDS/PAGE in this work used a gradient polyacrylamide gel (10–20%). All data shown in the present study were measured at least in triplicate.

ACKNOWLEDGMENTS. We thank our colleagues Drs. T. Hisabori, N. Mitome, P. Kahar, and M. Fujikawa for helpful discussion; and Mrs. J. Suzuki, T. Kamita, and A. Tatsuguchi for excellent technical assistance.

¶Plasmid pTRN-ASDS is a derivative of pTR19-ASDS (10). In the plasmid, its *lac* operator regulation system does not function by unknown mutation, and therefore, the gene introduced is strongly expressed without an inducer, isopropyl-β-thiogalactopyranoside.

1. Boyer PD (2002) *J Biol Chem* 277:39045–39061.
2. Yoshida M, Muneyuki E, Hisabori T (2001) *Nat Rev Mol Cell Biol* 2:669–677.
3. Girvin ME, Fillingame RH (1993) *Biochemistry* 32:12167–12177.
4. Stock D, Leslie AG, Walker JE (1999) *Science* 286:1700–1705.
5. Mitome N, Suzuki T, Hayashi S, Yoshida M (2004) *Proc Natl Acad Sci USA* 101:12159–12164.
6. Vonck J, von Nidda TK, Meier T, Matthey U, Mills DJ, Kuhlbrandt W, Dimroth P (2002) *J Mol Biol* 321:307–316.
7. Seelert H, Poetsch A, Dencher NA, Engel A, Stahlberg H, Muller DJ (2000) *Nature* 405:418–419.
8. Diez M, Zimmermann B, Borsch M, Konig M, Schweinberger E, Steigmiller S, Reuter R, Felekyan S, Kudryavtsev V, Seidel CA, Graber P (2004) *Nat Struct Mol Biol* 11:135–141.
9. Ueno H, Suzuki T, Kinosita K, Jr, Yoshida M (2005) *Proc Natl Acad Sci USA* 102:1333–1338.
10. Suzuki T, Ueno H, Mitome N, Suzuki J, Yoshida M (2002) *J Biol Chem* 277:13281–13285.
11. Stahlberg H, Muller DJ, Suda K, Fotiadis D, Engel A, Meier T, Matthey U, Dimroth P (2001) *EMBO Rep* 2:229–233.
12. Laubinger W, Dimroth P (1988) *Biochemistry* 27:7531–7537.
13. Neumann S, Matthey U, Kaim G, Dimroth P (1998) *J Bacteriol* 180:3312–3316.
14. Matthey U, Kaim G, Dimroth P (1997) *Eur J Biochem* 247:820–825.
15. Gay NJ, Walker JE (1981) *Nucleic Acids Res* 9:3919–3926.
16. Gay NJ, Walker JE (1981) *Nucleic Acids Res* 9:2187–2194.
17. Downie JA, Langman L, Cox GB, Yanofsky C, Gibron F (1980) *J Bacteriol* 143:8–17.
18. Porter AC, Brusilow WS, Simoni RD (1983) *J Bacteriol* 155:1271–1278.
19. Brusilow WS, Porter AC, Simoni RD (1983) *J Bacteriol* 155:1265–1270.
20. von Meyenburg K, Jorgensen BB, Nielsen J, Hansen FG (1982) *Mol Gen Genet* 188:240–248.
21. Gay NJ (1984) *J Bacteriol* 158:820–825.
22. Schneppe B, Deckers-Hebestreit G, Altendorf K (1990) *J Biol Chem* 265:389–395.
23. Solomon KA, Hsu DK, Brusilow WS (1989) *J Bacteriol* 171:3039–3045.
24. Schneppe B, Deckers-Hebestreit G, Altendorf K (1991) *FEBS Lett* 292:145–147.
25. Gerike U, Dimroth P (1994) *Arch Microbiol* 161:495–500.
26. Kaim G, Ludwig W, Dimroth P, Schleifer KH (1992) *Eur J Biochem* 207:463–470.
27. Ohta S, Yohda M, Ishizuka M, Hirata H, Hamamoto T, Otawara-Hamamoto Y, Matsuda K, Kagawa Y (1988) *Biochim Biophys Acta* 933:141–155.
28. Revington M, McLachlin DT, Shaw GS, Dunn SD (1999) *J Biol Chem* 274:31094–31101.
29. Kaim G, Dimroth P (1993) *Eur J Biochem* 218:937–944.
30. Laubinger W, Dimroth P (1989) *Biochemistry* 28:7194–7198.
31. Ackerman SH, Tzagoloff A (1990) *J Biol Chem* 265:9952–9959.
32. Tzagoloff A, Barrientos A, Neupert W, Herrmann JM (2004) *J Biol Chem* 279:19775–19780.
33. Osman C, Wilmes C, Tatsuta T, Langer T (2007) *Mol Biol Cell* 18:627–635.
34. Zeng X, Neupert W, Tzagoloff A (2007) *Mol Biol Cell* 18:617–626.
35. Altamura N, Capitanio N, Bonnefoy N, Papa S, Dujardin G (1996) *FEBS Lett* 382:111–115.
36. van Bloois E, Jan Haan G, de Gier JW, Oudega B, Luirink J (2004) *FEBS Lett* 576:97–100.
37. van der Laan M, Bechtluft P, Kol S, Nouwen N, Driessen AJ (2004) *J Cell Biol* 165:213–222.
38. Laubinger W, Deckers-Hebestreit G, Altendorf K, Dimroth P (1990) *Biochemistry* 29:5458–5463.
39. Monticello RA, Angov E, Brusilow WS (1992) *J Bacteriol* 174:3370–3376.
40. Suzuki T, Murakami T, Iino R, Suzuki J, Ono S, Shirakihara Y, Yoshida M (2003) *J Biol Chem* 278:46840–46846.
41. von Ballmoos C, Dimroth P (2004) *Anal Biochem* 335:334–337.